A Modified Double-Integral-Sliding-Mode-Controller for a Microgrid System With Uncertainty

Swati Sucharita Pradhan and Raseswari Pradhan*

[1]*Dept. of Electrical Engg., VSSUT Burla, Sambalpur, India*
E-mail: swati89pradhan@gmail.com; rase1512@gmail.com
**Corresponding Author*

Received 20 July 2020; Accepted 29 September 2020;
Publication 08 December 2020

Abstract

Recently infiltration of large scale of microgrid systems into the power grid is recorded. Among these systems, photovoltaic (PV) based microgrid systems are more in demand due to its renewable, pollution free properties and abundantly available fuel. Grid integration of this microgrid system again enhanced its energy efficiency. But, dynamics of this PV based microgrid system is highly nonlinear and uncertain in nature. It suffers from parametric uncertainties. This kind of system can't be controlled properly by conventional linear controllers. Sliding mode controller (SMC) is capable of controlling this kind of system with ease. However, SMC suffers from its inherent chattering introduction in the system output waveform. To reduce the chattering from the output waveform, there is requirement of some modification in the existing SMC structure dynamics. This paper presents an extended state observer based double integral sliding mode controller (DISMC) for this studied system. By using DISMC, the chattering magnitude is diminished greatly. Parameter uncertainties of the system lead to some unknown control states. These unknown states are identified by the state observer. Therefore, the proposed controller is more efficient in reference tracking, disturbance

Distributed Generation & Alternative Energy Journal, Vol. 35_1, 19–46.
doi: 10.13052/dgaej2156-3306.3512

rejection and robust stability. To test the efficacies of the proposed controller, results of the studied system with this controller are compared with that of H_∞ controller.

Keywords: Three-phase microgrid, photovoltaic system, DISMC, H_∞ controller, parametric uncertainties.

1 Introduction

PV based microgrid systems have emerged as a reliable and efficient source of power generation in recent times. This happened as a result of manufacturing cost reduction of the PV module and the use of more efficient power electronic converters which improves the overall system efficiency and reliability [1]. The PV systems generally are of standalone or grid connected types. The later type of system is again of two types such as single-stage and two-stage types. Although two stage PV systems are more in use conventionally due to its simplicity, it has the demerit of reducing the overall systems efficiency besides increasing the cost [2]. For this reason, the single-stage PV system is preferably in demand now-a-days. Here, the inverter performs dual functions like tracking of maximum power from PV panel and regulation of dc-link voltage. With a suitable filter it is also capable of providing sinusoidal current to the grid [3].

In this system, magnitude and quality of input power depend on environment. Environmental conditions are always stochastic in nature. Therefore, the input power of the system is inherently nonlinear. Further nonlinearity factors are added by the power electronics switches of dc to dc converters and inverters. Thus, the linear controllers like PID-controller are unable to handle this system efficiently. To make them usable, the system needs to be linearized near the desired operating point. However, change in equilibrium point may leads to system failure [4]. Again, this controller needs the system structure data in regular time-span for tuning its gains [5]. These nonlinearities can be cancelled by using feedback linearization techniques. However, these controllers are very sensitive to any change of parameters [6, 7]. It also aggravates the complication in modeling and execution of the inverter [8].

Linear controllers are conventional and ease in usage. Hence, they are widely used in industrial applications. However, they fail in presence of parameter uncertainties [9]. In these situations, a nonlinear controller like H_∞ controller can be applied. But, the dynamics of H_∞ controller is very complex to design and implement [10]. Since the input to the PV system is

highly stochastic in nature and the overall system is also being nonlinear, use of this H_∞ controller further enhance complexity without much gain in performance. It is also silent about the stability aspects. Therefore, there is a need of a controller which has the characteristics of robustness and maintains system stability in any condition [11].

SMC is one of the non-linear controllers that is inherently robust and maintain stability in all condition. This controller is easy to implement also [11]. However, one major problem with SMC is the introduction of steady state error in regulation due to its limited switching frequency [12]. To decrease this steady state error, one of the potential solutions is to increase the order of the controller [13]. SMC has been widely used in PV system in both standalone and grid connected system [14]. But the use of higher order SMC in particular the double integral sliding mode controller (DISMC) application has only been limited to that of in MPPT control standalone PV systems [15]. But its implementation in PV system tied with grid has not been investigated in the past. Again, sliding mode-based controllers are dependent on system dynamics and state variables are vital in their formulation. However, in many cases, some or all states of the system are unknown. In that case, observers can be used to estimate the unknown states [16, 17].

The contributions of this paper are as follows. A hybrid extended state observer based DISMC controller is proposed for the regulation of dc link voltage and grid current respectively. DISMC is based on the information of all the states of the studied PV system. The state observer provides information about the unknown control states that are lost due to presence of parameter uncertainties of the system. The results of the studied PV system are compared with that of the SMC and H-∞ controllers.

This paper is organized as follows. Section 2 designates the mathematical modeling of the studied PV system. Problem formulation is done in Section 3. Then Section 4 discusses the structure of the hybrid controller. Further simulation results and corresponding discussion are in Section 5. Finally, the concluding remarks are in Section 6.

2 System Modelling

The overall layout of the studied PV system is shown in Figure 1. The studied power system consists of following major components (i) PV array, (ii) DC-link, (iii) Voltage Source Inverter (VSI), (iv) Grid filter and (v) Grid. This power system has PV panels as input. The input supply is provided to the ac grid using an intermediate 3-ϕ inverter. Here the inverter performs the dual

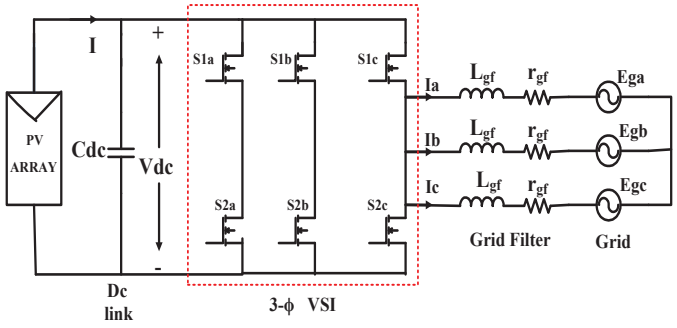

Figure 1 Three phase grid integrated PV system.

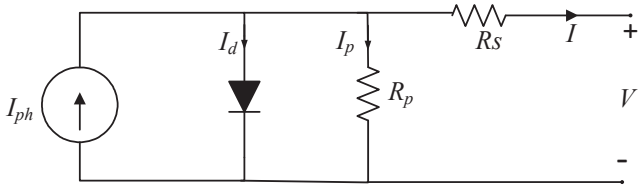

Figure 2 Equivalent circuit representation of a PV panel model.

tasks such as maintain the input voltage from solar panel at its maximum level and maintaining required level of active and reactive power by regulating the current injected to the grid.

PV cell is the vital component of a solar power system. Therefore, it is required to use an appropriate model of it. From widely available models, Figure 2 shows the widely accepted one model of a PV cell. Here, V and I are the voltage and current generated from a PV panel model respectively. It also consists of N_p and N_s are the number of parallel and series connected modules to increase the array voltage and current respectively. Thus the overall array current is given as follows.

$$I = N_p I_{ph} - N_p I_o \left[\exp\left\{\frac{q}{AkT}\left(\frac{V}{N_s} + \frac{IR_s}{N_p}\right)\right\} - 1\right] - \frac{N_p}{R_p}\left(\frac{V}{N_s} + \frac{IR_s}{N_p}\right) \tag{1}$$

The inverter output voltages which are input to the grid is given as below.

$$V_a = Lgf\frac{di_a}{dt} + i_a rgf + E_a$$

$$V_b = Lgf\frac{di_b}{dt} + i_b rgf + E_b \tag{2}$$
$$V_c = Lgf\frac{di_c}{dt} + i_c rgf + E_c$$

Let, S_{1a}, S_{1b}, S_{1c}, S_{2a}, S_{2b}, S_{2c} be the switching signals fed to the inverter and $S_{1a} = S_{2b} = S_a$, $S_{1b} = S_{2b} = S_b$, $S_{1c} = S_{2c} = S_c$. Further, the voltage across the inverter is given as follows.

$$V_a = \frac{V}{3}(2S_a - S_b - S_c)$$
$$V_b = \frac{V}{3}(-S_a + 2S_b - S_c) \tag{3}$$
$$V_c = \frac{V}{3}(-S_a - S_b + 2S_c)$$

Analyzing Equations (2) and (3), the following set of equations are generated.

$$\frac{di_a}{dt} = \frac{-rgf}{Lgf}i_a - \frac{1}{Lgf}E_a + \frac{V_{pv}}{3Lgf}(2S_a - S_b - S_c)$$
$$\frac{di_b}{dt} = \frac{-rgf}{Lgf}i_b - \frac{1}{Lgf}E_b + \frac{V_{pv}}{3Lgf}(-S_a + 2S_b - S_c) \tag{4}$$
$$\frac{di_c}{dt} = \frac{-rgf}{Lgf}i_c - \frac{1}{Lgf}E_c + \frac{V_{pv}}{3Lgf}(-S_a - S_b + 2S_c)$$

Here, Equations (4) and (5) represent the overall model of the studied system. Again, voltage (V_{dc}) across the dc link capacitor (C_{dc}) is formulated as follows.

$$\frac{dV_{pv}}{dt} = \frac{dV_{dc}}{dt} = \frac{1}{Cdc}[i_{pv} - (i_{inv})] \tag{5}$$

Where the inverter input current

$$i_{inv} = i_a S_a + i_b S_b + i_c S_c \tag{6}$$

It is observed that the model is nonlinear because of the switching signals and i_{pv} and also time variant time in nature. This model is very complex to analyze and control. Therefore, to enhance easiness of the model, it is remodeled in time invariant dqo reference frame rotating at angular frequency (ω) of grid as shown in Equation (7). In this equation, the applied voltage and

current terms bears the usual terms of current and voltages in their respective dqo reference frame.

$$\frac{d}{dt}\begin{bmatrix} i_d \\ i_q \\ V_{pv} \end{bmatrix} = \begin{bmatrix} -\frac{r_{gf}}{L_{gf}} & w & \frac{S_d}{L_{gf}} \\ -w & -\frac{r_{gf}}{L_{gf}} & \frac{S_q}{L_{gf}} \\ -\frac{S_d}{C_{dc}} & -\frac{S_q}{C_{dc}} & 0 \end{bmatrix} \begin{bmatrix} i_d \\ i_q \\ V_{pv} \end{bmatrix} + \begin{bmatrix} -\frac{1}{L_{gf}} & 0 & 0 \\ 0 & -\frac{1}{L_{gf}} & 0 \\ 0 & 0 & \frac{1}{C_{dc}} \end{bmatrix} + \begin{bmatrix} E_d \\ E_q \\ i_{pv} \end{bmatrix} \tag{7}$$

3 Uncertain and Nonlinear Photovoltaic System

Some uncertain and nonlinear factors may be intentionally or unintentionally excluded from the mathematical model of the PV dynamics. This creates remarkable differences between outputs of the real system and the modeled system. To make the modeled system more realistic some of its uncertainty factors need to be added to the modeled system dynamics. Further, system efficiency and stability would be enhanced if controllers are designed referring this dynamic [18].

In the studied PV system, the grid line parameters like inductance, resistance and the capacitance may suffers from various nonlinearities and uncertainties. So, their values are to be approximated near to their actual values. The approximated line parameters are shown as follows.

$$L = L_{nom}(1 + (\rho_L + \alpha)\Delta_L) \tag{8}$$

$$R = R_{nom}(1 + \rho_R \Delta_R) \tag{9}$$

$$C = C_{nom}(1 + (\rho_C + \beta)\Delta_C) \tag{10}$$

Where L_{nom}, R_{nom} and C_{nom} are the nominal values of the respective line parameters as inductance (L), resistance (R), and capacitance (C) respectively. Similarly, ρ_L, ρ_R, ρ_C and $\Delta_L, \Delta, \Delta_C$ are the possible uncertain and

nonlinear factors of introduced to these parameters. Again, the line parameters can be presented in linear fractional transformation (LFT) structure so as to introduce the above uncertainties and nonlinearities to the studied system model [18]. First, the inductor in LFT form is represented as follows

$$\frac{1}{L} = \frac{1}{L_{nom}} - \frac{\rho_L + \alpha}{L_{nom}} \Delta_L (1 + \rho_L + \alpha)\Delta_L)^{-1} = F_U(M_L, \Delta_L) \tag{11}$$

Where

$$M_L = \begin{bmatrix} -(\rho_L + \alpha) & \dfrac{1}{L_{nom}} \\ -(\rho_L + \alpha) & \dfrac{1}{L_{nom}} \end{bmatrix} \tag{12}$$

Similarly, the other parameters in LFT forms are shown as follows.

$$R = R_{nom}(1 + \rho_R \Delta_R) = F_u(M_R, \Delta_R) \tag{13}$$

$$C = C_{nom}(1 + (\rho_C + \beta)\Delta_C) = F_U(M_C, \Delta_C) \tag{14}$$

Where,

$$M_R = \begin{bmatrix} 0 & R_{nom} \\ \rho_R & R_{nom} \end{bmatrix} \quad \text{and} \quad M_c = \begin{bmatrix} 0 & C_{nom} \\ \rho_C + \beta & C_{nom} \end{bmatrix} \tag{15}$$

The block diagram of the studied system with parameters in LFT is shown in Figure 3. Here y_L, y_R, y_C and u_L, u_R, u_C are the inputs and outputs from the uncertainty block Δ_L, Δ_R and Δ_C respectively.

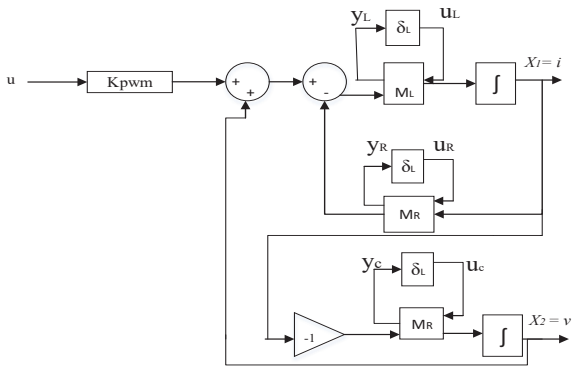

Figure 3 Block diagram of the studied nonlinear system with uncertain parameters.

Assuming all these uncertainty as parameters d1 and d2 for state equation corresponding to id and iq, now Equation (7) can be rewritten as follows.

$$\begin{bmatrix} \dot{x}_1 \\ \dot{x}_2 \\ \dot{x}_3 \end{bmatrix} = \begin{bmatrix} f_1(x_1,t) \\ f_2(x_2,t) \\ a_3 x_3 \end{bmatrix} + \begin{bmatrix} g_1(x_1,t) \\ g_2(x_2,t) \\ b_3 \end{bmatrix} \begin{bmatrix} u_1 \\ u_2 \\ u_3 \end{bmatrix} \tag{16}$$

Where,

$$\begin{bmatrix} x_1 \\ x_2 \\ x_3 \end{bmatrix} = \begin{bmatrix} i_d \\ i_q \\ V_{pv} \end{bmatrix}, \begin{bmatrix} u_1 \\ u_2 \\ u_3 \end{bmatrix} = \begin{bmatrix} E_d \\ E_q \\ i_{pv} \end{bmatrix},$$

$$\begin{bmatrix} f_1(x_1,t) \\ f_2(x_2,t) \\ a_3 x_3 \end{bmatrix} = \begin{bmatrix} -\frac{r_{gf}}{L_{gf}} & w & \frac{S_d}{L_{gf}} \\ -w & -\frac{r_{gf}}{L_{gf}} & \frac{S_q}{L_{gf}} \\ -\frac{S_d}{C_{dc}} & -\frac{S_q}{C_{dc}} & 0 \end{bmatrix} \begin{bmatrix} i_d \\ i_q \\ V_{pv} \end{bmatrix} + \begin{bmatrix} d1 \\ d2 \\ 0 \end{bmatrix} \tag{17}$$

4 Problem Formulation

In a three phase system the active power P and the reactive power Q are given by [16].

$$P = \frac{3}{2}(v_d i_d + v_q i_q)$$
$$Q = \frac{3}{2}(v_d i_q - v_q i_d) \tag{18}$$

Assuming the three phase grid voltage to be sinusoidal, the grid voltage vector v_q=0. Hence the active and reactive power

$$P = \frac{3}{2} v_d i_d$$
$$Q = \frac{3}{2} v_d i_q \tag{19}$$

Hence the powers, P and Q can be controlled by controlling the currents i_d and i_q respectively. For this the grid current in dq-frame is made to track the reference currents id_{ref} and iq_{ref}. Further, the system power factor is required to be maintained unity as it is integrated to utility system. For that the reference i_q given to the controller should be 0.

5 Proposed Controller Design

The detail formulation of the two controllers is as follows.

5.1 Extended State Observer Design

A nonlinear extended state observer is included to estimate the unknown parameters d1 and d2 [17]. This observer is designed based on hyperbolic tangent function. It is assumed that, due to the presence of uncertainties in the system, the states x_1 and x_2 are not fully known. Let's consider one parallel system that is represented by state variables Z_1 and Z_2. Here, Z_1 and Z_2. Give us the estimated values of x_1 and x_2 by the state observer.

$$\begin{aligned} \dot{Z}_1 &= -a_1 \tanh(b_1(Z_1 - x_1) \\ \dot{Z}_2 &= -a_2 \tanh(b_2(Z_1 - x_2) \end{aligned} \tag{20}$$

For this system, the estimated errors are calculated as follows.

$$\begin{aligned} e_1 &= d_1 - Z_1 \\ e_2 &= d_2 - Z_2 \end{aligned} \tag{21}$$

$$\begin{aligned} d_1 &= e_1 + Z_1 \\ d_2 &= e_2 + Z_2 \end{aligned} \tag{22}$$

These estimated errors also bounded for bounded input.

5.2 DISMC Controller

The algorithm for the design of DISMC for grid connected PV system is as per the following steps.

Step 1: Estimation of reference current id, id_{ref} from the output of the PI controller and initializing $I_{qref} = 0$.

Step 2: Designing the sliding surfaces S1 and S2 for regulating current id and iq respectively in the following structures.

$$\begin{aligned} S_1 &= a_d X_{1d} + b_d X_{2d} + c_d X_{3d} + d1 \\ S_2 &= a_q X_{1q} + b_q X_{2q} + c_q X_{3q} + d2 \end{aligned} \tag{23}$$

Where,

$$X_{1d} = id_{ref} - id,$$

$$
\begin{aligned}
X_{2d} &= \int (id_{ref} - id)dt, \\
X_{3d} &= \int \left[\int (id_{ref} - id)dt \right] dt \\
X_{1q} &= iq_{ref} - iq, \\
X_{2q} &= \int \big(iq_{ref} - iq\big)dt, \\
X_{3q} &= \int \left[\int \big(iq_{ref} - iq\big)dt \right] dt
\end{aligned} \tag{24}
$$

Where a_d, b_d, c_d and a_q, b_q, c_q are the coefficients of the sliding surfaces S_1 and S_2 respectively.

Figure 4 shows the layout of the proposed control set-up. Here, a nonlinear estimated state-observer based on hyperbolic tangent function is presented for estimating disturbance mismatching (d1 and d2). After that the sliding surface of the proposed DISMC is calculated. Then, the required control law is computed.

Step 3: Next step is the design of control inputs, u which satisfies the sliding mode existence law. The control input *u* drives the state variables to the sliding surface and maintains them on the surface thereafter irrespective of any disturbance.

The control input u is the addition of equivalent control input u_{eq} and nonlinear control input U_n.

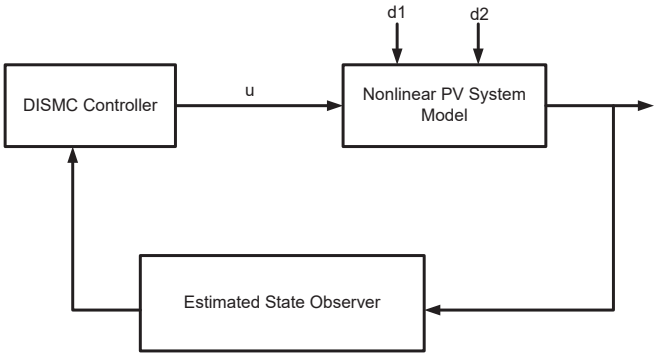

Figure 4 Layout of proposed control setup.

Step 4: Calculation of the equivalent control input ud_{equ} and uq_{equ} obtained by using the invariance condition as follows.

$$\begin{aligned}
&\dot{S1} = 0 \quad \text{at } ud = ud_{equ} + d1 \\
&\dot{S2} = 0 \quad \text{at } uq = uq_{equ} + d2 \\
&a\left[\frac{d}{dt}(id_{ref}) - \left[\frac{-R_{gf}}{L_{gf}}id + wiq + \frac{ud_{equ}}{L_{gf}} - \frac{1}{L_{gf}}Ed\right]\right. \\
&\quad \left. + b\,(id_{ref} - id) + c\int (id_{ref} - id)\,dt = 0\right. \qquad (25)
\end{aligned}$$

solving the above equation, we obtain

$$\begin{aligned}
ud_{equ} = &\left[L_{gf}\frac{d}{dt}(id_{ref}) + R_{gf}id - L_{gf}wiq\right] + Ed + \alpha_d L_{gf}(id_{ref} - id) \\
&+ \beta_d L_{gf}\int (id_{ref} - id)dt \qquad (26)
\end{aligned}$$

Similarly, we can obtain

$$\begin{aligned}
uq_{equ} = &\left[L_{gf}\frac{d}{dt}(iq_{ref}) + R_{gf}iq + L_{gf}wiq\right] \\
&+ Eq + \alpha_q L_{gf}(iq_{ref} - iq) + \beta_q L_{gf}\int (iq_{ref} - iq)dt \qquad (27)
\end{aligned}$$

Step 5: The nonlinear control inputs can be chosen as

$$\begin{aligned}
ud_n &= sgn(S1) \\
uq_n &= sgn(S2) \qquad (28)
\end{aligned}$$

Step 6: Hence the control inputs to the inverter are

$$\begin{aligned}
Ud = &\left[L_{gf}\frac{d}{dt}\,(id_{ref}) + R_{gf}id - L_{gf}wiq\right] \\
&+ Ed + \alpha_d L_{gf}\,(id_{ref} - id) + \beta_d L_{gf}\int (id_{ref} - id)\,dt + sgn\,(S1) \qquad (29)
\end{aligned}$$

$$\begin{aligned}
Uq = &\left[L_{gf}\frac{d}{dt}\left(iq_{ref}\right) + R_{gf}iq + L_{gf}wiq\right] \\
&+ Eq + \alpha_q L_{gf}\left(iq_{ref} - iq\right) + \beta_q L_{gf}\int \left(iq_{ref} - iq\right)dt + sgn(S2) \qquad (30)
\end{aligned}$$

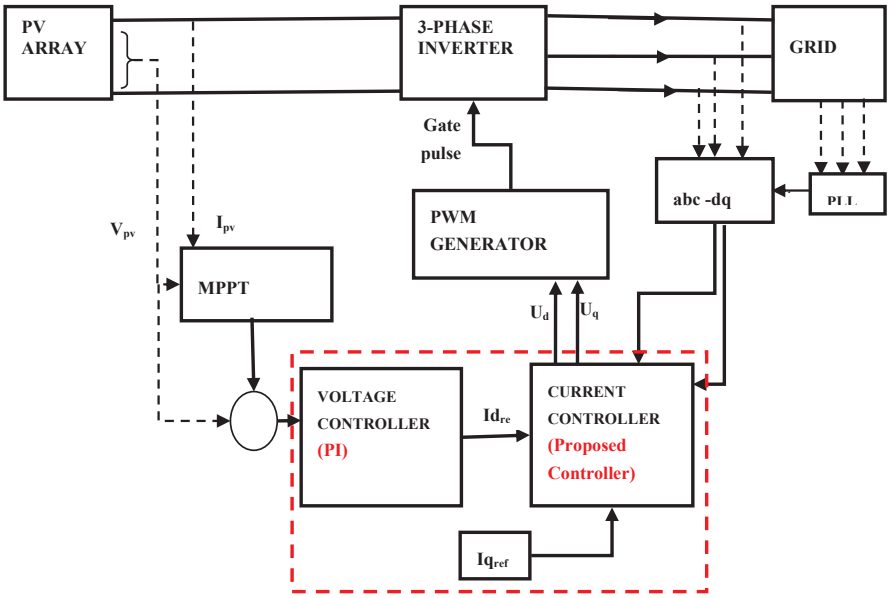

Figure 5 Layout of the Studied Power System with controller.

The detailed controller model of the studied system is shown using Figure 5.

6 Results and Discussions

Sunpower SPR-415E-WHT-D PV modules are used in the software simulation. The parameters of the system are shown in Table 1. The proposed three phase system is analyzed and controlled with simulation results. The MATLAB/SIMULINK model of the studied system is shown using Figure 6.

The simplified input-output block diagram is shown in Figure 7. Here, gain of the block G_{pv} is taken as follows.

$$G_{pv} = \begin{bmatrix} A & B_1 & B_2 \\ C_1 & D_{11} & D_{12} \\ C_2 & D_{21} & D_{22} \end{bmatrix} \tag{31}$$

Where

$$A = \begin{bmatrix} \frac{-R_{nom}}{L_{nom}} & \frac{1}{L_{nom}} \\ -C_{nom} & 0 \end{bmatrix},$$

Table 1 Proposed system parameters

	Parameters	Values
PV	Voltage at MPP(V)	72.9
	Current at MPP (A)	5.69
	Np	100
	Ns	7
	Rp (ohms)	419.78
	Rs (ohms)	0.5371
Grid	Grid voltage (KV)	25
	Line inductance L(mH)	0.4
	Line resistance R (ohms)	0.01
	Frequency (Hz)	50
DC link	Voltage Vdc(V)	480

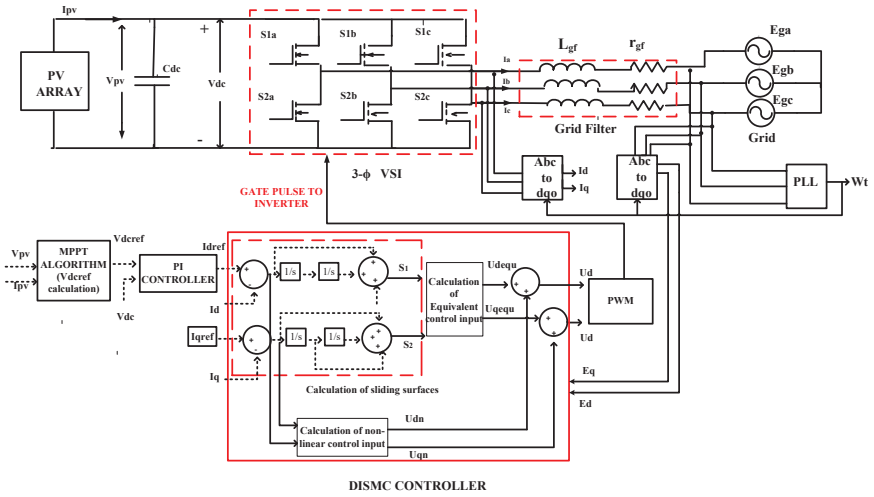

Figure 6 Detailed model of proposed controller.

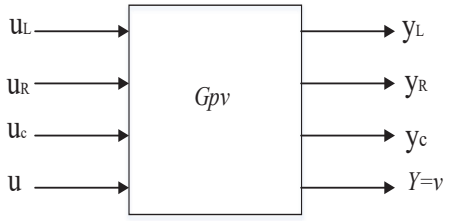

Figure 7 Input–output block diagram of studied system.

$$B_1 = \begin{bmatrix} -(\rho_L + \alpha) & \dfrac{-\rho_R}{R_{nom}} & 0 \\ 0 & 0 & (\rho_c + \beta) C_{nom} \end{bmatrix}$$

$$B_2 = \begin{bmatrix} \frac{K_{pwm}}{L_{nom}} \\ 0 \end{bmatrix}$$

$$C_1 = \begin{bmatrix} \dfrac{-R_{nom}}{L_{nom}} & \dfrac{1}{L_{nom}} \\ R_{nom} & 0 \\ -C_{nom} & 0 \end{bmatrix}$$

$$D_{11} = \begin{bmatrix} -(\rho_L + \alpha) & -\dfrac{\rho_R}{L_{nom}} & 0 \\ 0 & 0 & 0 \\ 0 & 0 & 0 \end{bmatrix}$$

$$D_{12} = \begin{bmatrix} \dfrac{K_{pwm}}{L_{nom}} \\ 0 \\ 0 \end{bmatrix}$$

$$C_2 = \begin{bmatrix} 0 & 1 \end{bmatrix}$$

$$D_{21} = \begin{bmatrix} 0 & 0 & 0 \end{bmatrix}, D_{22} = 0$$

In this work, the uncertain and nonlinear factors are assumed as follows. $\rho_L = 0.4, \rho_R = 0.2$, $\rho_C = 0.3$ and also $-1 \leq \Delta_L, \Delta_R, \Delta_C \leq 1$. The nominal values of L, R and C are taken as 2 H, 30Ω and 50μF respectively.The studied system with upper LFT is shown in Figure 8.

The PV characteristic of the studied PV modules is shown in Figure 9(a). The voltage at MPP, V_{mpp} in our case is around 515Volts. Here, the MPPT is maintaining the array voltage at its peak. The measured array voltage is shown in Figure 9(b). In Figure 9(c), it can be seen that the both voltage and current of the grid are maintained in phase as per our objective. This indicates that the system is functioning at unity power factor and hence the proposed system is fulfilling one of our design objective like keeping voltage and current of utility at unity power factor.

For better explanation of the efficacy of the proposed controller, the output results of the studied PV system with the proposed controller is compared with that of the system with that of the H∞ controller. The reason behind

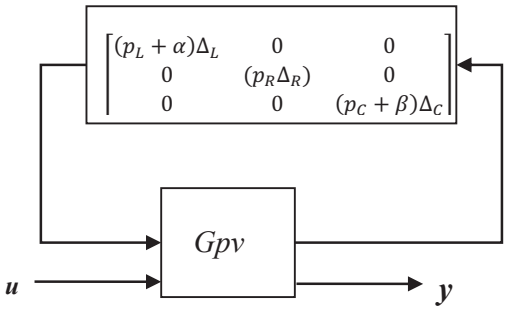

Figure 8 Studied system with LFT parameters.

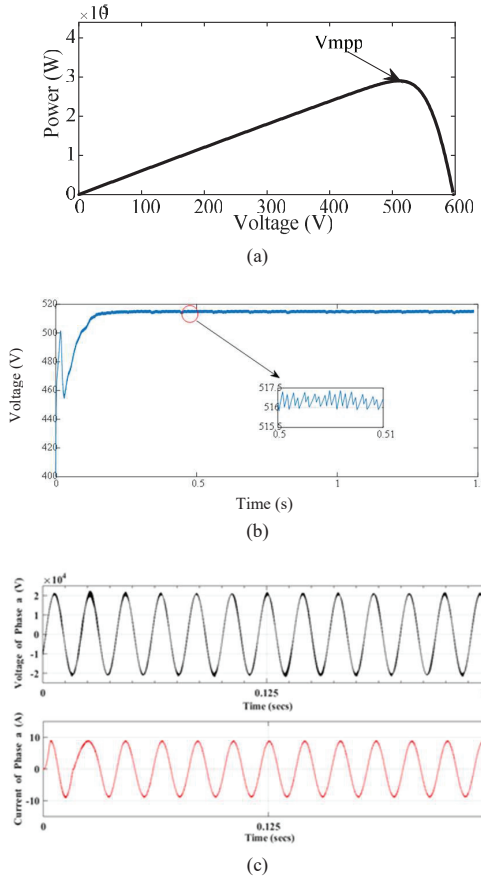

Figure 9 (a) Grid Voltage and grid current of phase a, (b) Measured V_{dc} and (c) Measured V_{dc}.

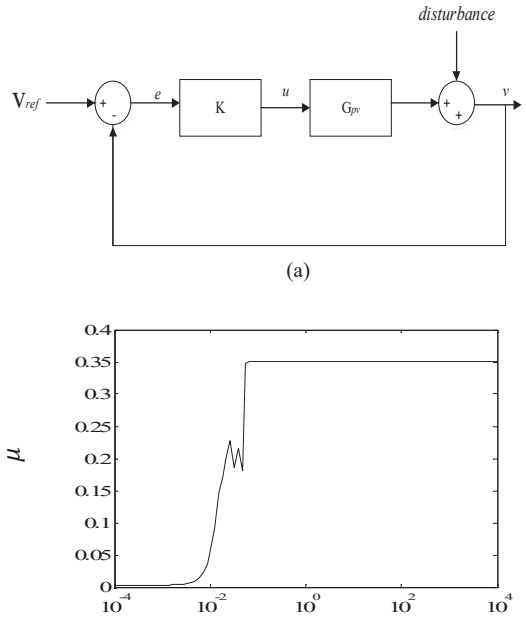

Figure 10 (a) Standard configuration of the studied system with H-∞ controller and (b) μ value for the studied system.

choosing H∞ controller for comparison is due to its capability of handling parameter uncertainty like the proposed controller. The block diagram of the studied system with H∞ controller is shown in Figure 10. For H∞ controller design, μ-based MATLAB tool-box (hinfsyn function) is used. Here, the weighing functions (W_1 and W_2) are chosen as follows to reduce control effort over high frequency range.

$$W_1 = 0.01\frac{s + 1.8}{s + 0.08} \tag{32}$$

and

$$W_2 = 0.05\frac{0.88s + 0.45}{0.9s + 0.65} \tag{33}$$

To get accurate reference tracking and disturbance rejection, the following condition is formulated from Equations (32) and (33) in all frequency

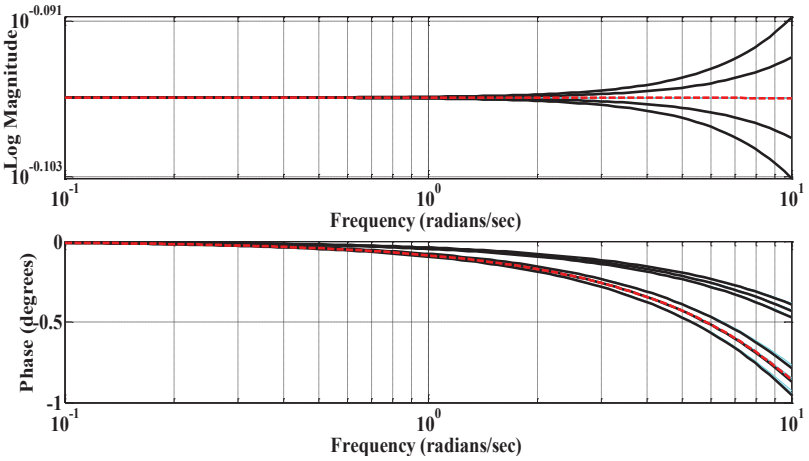

Figure 11 Bode plot of the perturbed open loop system.

ranges.

$$\sigma[S(jw)] < |1/W_1(jw)| \tag{34}$$

In H∞ controller design, the controller transfer function is obtained as a fourth order dynamics with a γ value of 1.0005 and a norm between 0.22499 and 0.22521. The controller obtained was found as follows.

$$K = \frac{-0.001s^3 - 0.2984s^2 - 0.2155s - 0.5678}{0.0001s^4 + 1.5001s^3 + 0.8871s^2 + 0.0614s + 0.001} \tag{35}$$

Further, another factor μ is introduced to test robustness of the studied system. Robust stability is guaranteed if the upper limit of μ is less than 1 ($\mu < 1$). The result showing μ is shown in Figure 10 (b). From Figure 10(b), it can be seen that for the proposed system μ value is settling at 0.35. So, the system is stable with the H∞ controller. Figure 11 is shows bode plot of the system for a wide range of solar irradiances from 200 W/m^2 to 1000 W/m^2 with a span of 200 W/m^2. It is seen that the system remains stable for all cases.

The robustness of the proposed controller is tested by changing the PV irradiance from 1000 G/m^2 to 800 G/m^2 at time t = 1 secs and again increased to 1000 W/m^2 at time t = 2 secs as shown in Figure 12(a). The grid current of phase a is compared with SMC as shown in Figure 12(b) and 12(c).

Figure 13(a) and (b) show the tracking behaviors of id and iq. Further the active and reactive component of current id and iq respectively are

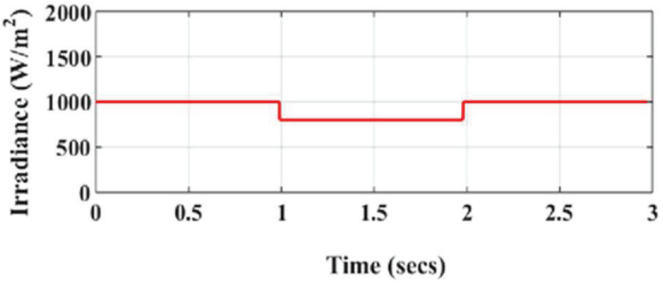

(a)

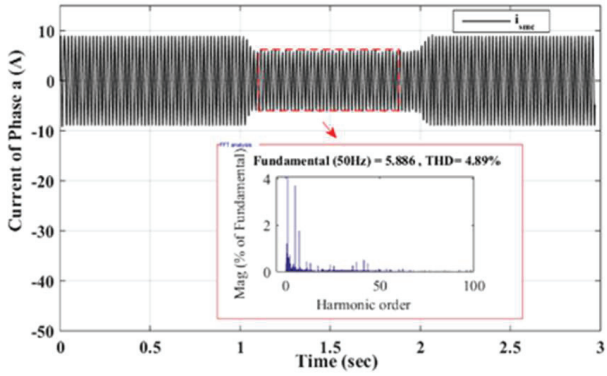

(b)

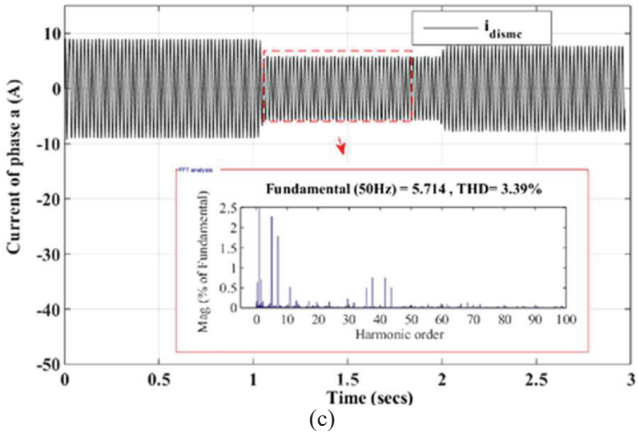

(c)

Figure 12 Current of phase a with change in irradiation using (a) SMC controller (b) proposed controller.

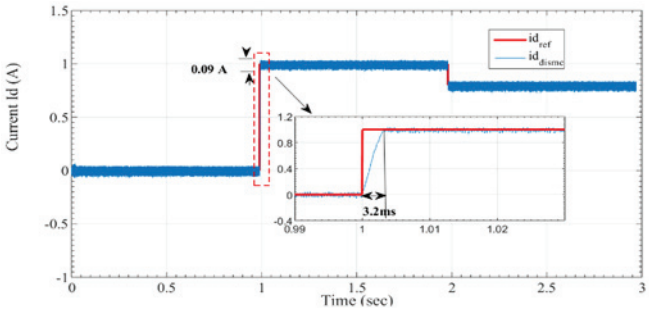

(a)

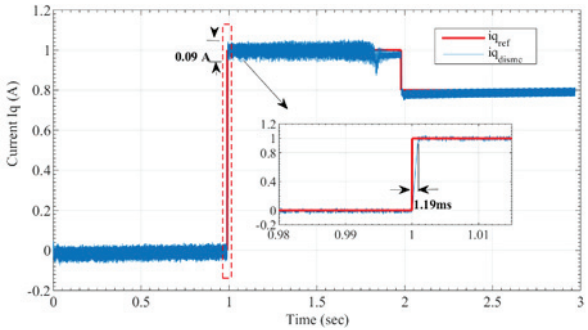

(b)

Figure 13 Reference tracking of (a) Id and (b) Iq using proposed controller.

changed to 1A at time t = 1 sec and then decreased to 0.8 A at time t = 2 secs It can be seen from Figure 13, that the current components id and iq track the respective reference currents id_{ref} and iq_{ref}. If this happens then automatically P and Q would be maintained at required levels. This ensures our second objective of the system design that is proper control of active and reactive power components P and Q respectively. Also, it is seen that when the irradiance is decreased from 1000 to 800 at time t = 1 sec, the THD of grid current in case of proposed controller is lesser than that of SMC. Hence the current fed will have less distortion and harmonic losses.

For analysis of the tracking performances of current id and iq in the variable irradiance scenario, the results in case of proposed controller are compared with that of SMC controller and H∞ controller. The tracking performances results in case of SMC controller are shown in Figure 14(a)

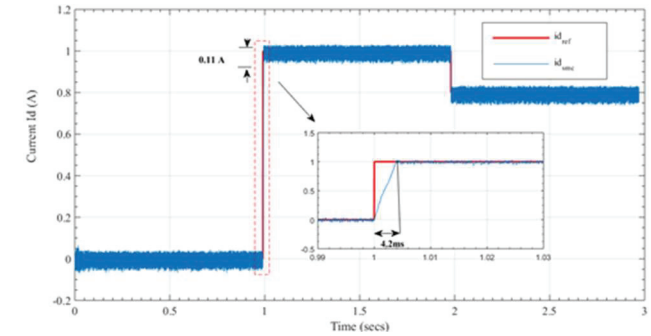

(a)

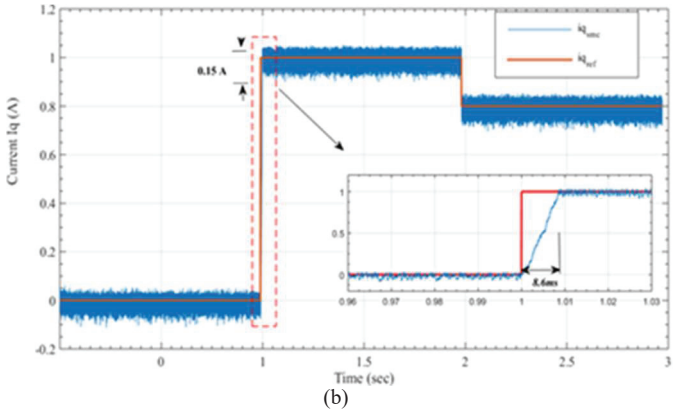

(b)

Figure 14 (a)Current id for change in id_{ref} and (b) current iqfor change in iq_{ref} using SMC controller.

and 14(b). Also, the behavior of current id and iq using the H∞ controller is shown in Figure 15(a) and 15(b). Comparing results of Figures 12–14, it is clear that the tracking is faster in case of the proposed controller (Figure 12). Further, the high frequency chattering is less in case of the proposed controller compared to that of H∞ controller and SMC controller. Therefore, it is seen that the proposed controller efficiently tracks both the reference currents generated in much lesser time than that of SMC and H∞ controller with least chattering. Hence, the system with the proposed controller experiences lesser transient losses.

Again, in Figure 16 the THD of the current fed to grid is also calculated in order to ensure that it is within the permissible limit which is 5 % as

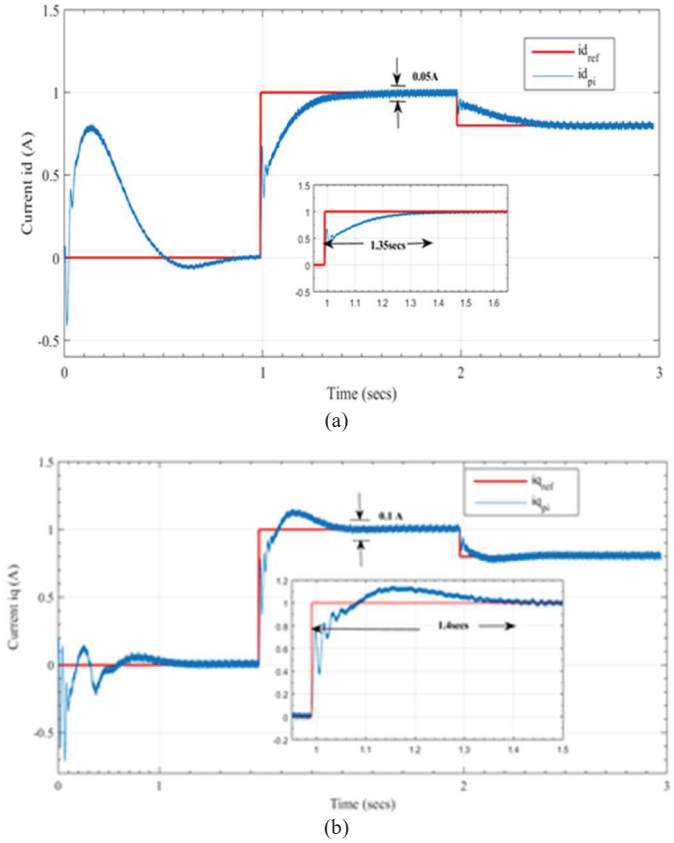

Figure 15 (a) Current id for change in id_{ref} and (b) current iq for change in iq_{ref} using H∞ controller.

recommended by grid codes. The THD was found to be 2.15% which is much lesser than that of the permissible limit.

The parameters of the proposed controller are selected so as to obtain the following behaviors such as (i) Minimum THD, (ii) lesser settling time for id and iq and (iii) Smaller chattering.

Tables 2 and 3 shows some of the chosen parameters and their corresponding output responses. The proposed controller is compared with H∞ and SMC controller in terms of its THD, chattering magnitude, Steady state error (SSE) and settling time in Table 4. The steady state error is calculated

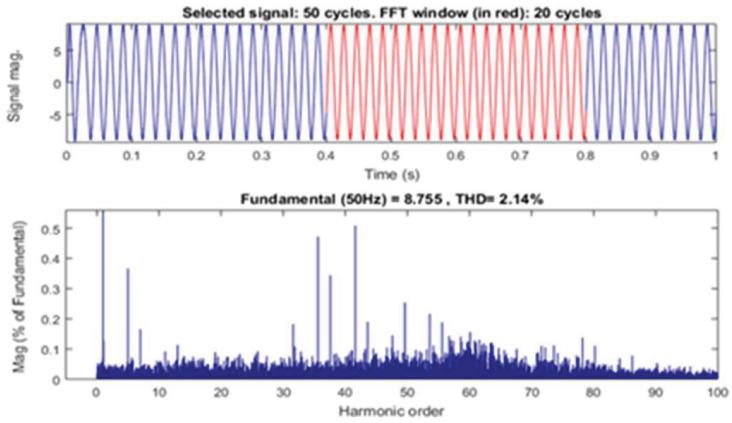

Figure 16 Total harmonic distortion of phase a grid current.

Table 2 Performance variation with THD and settling-time in case of different parameter selection Of DISMC controller

Parameters				THD in Phase a Grid Current (%)	Settling Time of Id (secs)	Settling Time of iq (secs)
α_d	β_d	α_q	β_q			
1	1	1	1	4.25	0.07sec	No reference tracking
1	1	1000	10000	3.98	0.07 sec	0.8
1	1	10000	10000	2.74	0.07 sec	1.4
1	1	50000	50000	2.17	0.07 sec	1.19×10^{-3}
10	1	50000	50000	2.19	1.01 sec	1.19×10^{-3}
12	0.1	50000	50000	2.14	3.2 msec	1.19×10^{-3}

Table 3 Performance variation with change in i_d and i_q in case of different parameter selection of DISMC controller

Parameters				$\Delta id = id_h - id_l$ (secs)	$\Delta iq = iq_h - iq_l$ (secs)
α_d	β_d	α_q	β_q		
1	1	1	1	0.15A	unstable
1	1	1000	10000	0.15A	0.18
1	1	10000	10000	0.15 A	0.32
1	1	50000	50000	0.15	0.09A
10	1	50000	50000	0.1	0.09
12	0.1	50000	50000	0.09 A	0.09A

Table 4 Overall comparison of simulation results

Parameters		H∞ Controller	SMC	PROPOSED Controller
Robust Stability		Not Present	Present	Present
Complexity		less	less	More
THD in grid current (%)		1.46	2.6	2.15
Chattering	Current Iq	0.1	0.15	0.09
Magnitude (A)	Current Id	0.05	0.11	0.09
SSE (%) during	Current Iq	0.4	2.5	0.5
reference tracking of	Current Id	0.5	1	0.5
Settling time	Current Iq	1.4	8.6×10^{-3}	1.19×10^{-3}
during change in reference (secs)	Current Id	1.35	4.2	3.2

as follows.

$$SSE_i = i_{ref-} \left[i_l + \frac{i_h - i_l}{2} \right] \tag{36}$$

Where i_{ref} = reference value of current
i_h = maximum value of current during steady state
i_l = minimum value of current during steady state

7 Conclusion

This paper proposes the simulation and control of a three phase photovoltaic system using an extended state observer based double integral sliding mode controller. The controller is usually a hybrid combination of two controllers. First one is used to regulate quality of power fed to the grid and maintained its power factor at unity. The second one is to make the PV array operate at its optimum point. Results shows both the active and reactive component of current are tracked efficiently thus maintaining the system at unity power factor. Also the system is tested for change in active and reactive current references Also the proposed controller is compared with a SMC and H∞ controller to test its robustness. It was found that the proposed controller has relatively lesser chattering magnitude, SSE and settling time than other

compared controllers. The studied system with the proposed controller is found to be inherently stable. Also, more accurate reference tracking and disturbance rejection can be maintained using this controller compared to SMC and H∞ controllers. It is further verified that the system remains stable in presence of uncertainty and nonlinearity.

References

[1] Erdem, Z. B. 2010. The contribution of renewable resources in meeting Turkey's energy-related challenges. Renewable and Sustainable Energy Reviews, 14(9): 2710–2722, doi: 10.1016/j.rser.2010.07.003.

[2] Jana, J., Saha, H., and Bhattacharya, K. D. 2017. A review of inverter topologies for single-phase grid-connected photovoltaic systems. Renewable and Sustainable Energy Reviews, 72: 1256–1270, doi: 10.1016/j.rser.2016.10.049.

[3] Kjaer, S. B., Pedersen, J. K., and Blaabjerg, F. 2005. A review of single-phase grid-connected inverters for photovoltaic modules. IEEE transactions on industry applications, 41(5): 1292–1306, doi: 10.1109/TIA.2005.853371.

[4] Eltawil, M. A., and Zhao, Z. 2010. Grid-connected photovoltaic power systems: Technical and potential problems—A review. Renewable and sustainable energy reviews, 14(1): 112–129, doi: 10.1016/j.rser.2009.07.015.

[5] Zue, A. O., and Chandra, A. 2009. State feedback linearization control of a grid connected photovoltaic interface with MPPT. In 2009 IEEE Electrical Power & Energy Conference (EPEC): 1–6, doi: 10.1109/EPEC.2009.5420870.

[6] Kim, I. S. 2007. Robust maximum power point tracker using sliding mode controller for the three-phase grid-connected photovoltaic system. Solar Energy, 81(3): 405–414, doi: 10.1016/j.solener.2006.04.005.

[7] Mahmud, M. A., Pota, H. R., Hossain, M. J., and Roy, N. K. 2013. Robust partial feedback linearizing stabilization scheme for three-phase grid-connected photovoltaic systems. IEEE Journal of photovoltaics, 4(1): 423–431, doi: 10.1109/JPHOTOV.2013.2281721.

[8] Hassaine, L., OLias, E., Quintero, J., and Salas, V. 2014. Overview of power inverter topologies and control structures for grid connected photovoltaic systems. Renewable and Sustainable Energy Reviews, 30: 796–807, doi: 10.1016/j.rser.2013.11.005.

[9] Rasool, A., Ahmad, F., & Šabanović, A. 2017. Voltage source converter control under unbalanced grid voltage conditions.XXVI International Conference on Information, Communication and Automation Technologies (ICAT): 1–6, doi: 10.1109/ICAT.2017.8171643.

[10] Tan, S. C., Lai, Y. M., and Chi, K. T. 2008. General design issues of sliding-mode controllers in DC–DC converters. IEEE Transactions on Industrial Electronics, 55(3): 1160–1174, doi: 10.1109/TIE.2007.909058.

[11] Kim, I. S. 2006. Sliding mode controller for the single-phase grid-connected photovoltaic system. Applied Energy, 83(10): 1101–1115, doi: 10.1016/j.apenergy.2005.11.004.

[12] Hace, A., Jezernik, K., and Sabanovic, A. 2007. SMC with disturbance observer for a linear belt drive. IEEE Transactions on Industrial Electronics, 54(6): 3402–3412, doi: 10.1109/TIE.2007.906130.

[13] Chowdhury, M. A., and Mahmud, M. A. 2014. Characteristics evaluation of a H∞ loop-shaping controller for a single-phase PV system.IEEE PES Asia-Pacific Power and Energy Engineering Conference (APPEEC): 1–6, doi: 10.1109/APPEEC.2014.7066115.

[14] Baranwal, M., Askarian, A., Salapaka, S., and Salapaka, M. 2018. A distributed architecture for robust and optimal control of DC microgrids. IEEE Transactions on Industrial Electronics, 66(4): 3082–3092, doi: 10.1109/TIE.2018.2840506.

[15] Wang, Y., Wu, Q., Yang, R., Tao, G., and Liu, Z. 2018. H∞ current damping control of DFIG based wind farm for sub-synchronous control interaction mitigation. International Journal of Electrical Power & Energy Systems, 98: 509–519, doi. 10.1016/j.ijepes.2017.12.003.

[16] Zhang, X. P., Rehtanz, C., and Pal, B. 2012. Flexible AC transmission systems: modelling and control. Springer Science & Business Media, doi: 10.1007/978-3-642-28241-6.

[17] Toloue, S. F., Kamali, S. H., and Moallem, M. 2019. Multivariable sliding-mode extremum seeking PI tuning for current control of a PMSM. IET Electric Power Applications, 14(3): 348–356, doi: 10.1049/iet-epa.2019.0033.

[18] Pradhan, S. S., R. Pradhan and B.Subudhi. 2019. Design and Analysis of an H∞ Controller for a Single Phase Grid Connected Photovoltaic System with Parametric Uncertainties. Second International Conference on Advanced Computational and Communication Paradigms (ICACCP), doi. 10.1109/ICACCP.2019.8882898.

[19] Pradhan, R. and B. Subudhi. 2012. A new digital double integral sliding mode maximum power point tracker for photovoltaic power generation application. IEEE Third International Conference on Sustainable Energy Technologies (ICSET): 183–188, doi. 10.1109/ICSET.2012.6357395.

Biographies

Swati Sucharita Pradhan is pursuing her Ph.D. degree in department of EE, VSSUT, Burla under the supervision of Dr. Raseswari Pradhan and Prof. B. Subudhi. She has her educational degrees like B.Tech. from BPUT and M.Tech. from VSSUT, Burla. Her research interests are design and control of renewable energy systems.

Raseswari Pradhan was born in Bargarh, Odisha, India. She got her Ph.D. degree in control system engineering from National Institute of Technology, Rourkela, India in 2014. She got her B.E. and M.E. degrees in electrical engineering from I.G.I.T., Sarang, Utkal University, Odisha and Jadavpur University, Kolkata, respectively. Currently she is serving as an Assistant Professor in the Department of Electrical Engineering, Veer Surendra Sai University of Technology, Burla, India. She has more than ten papers

published in various reputed journals like IEEE Transactions on Sustainable Energy, IEEE Transactions on Control Systems Technology, IET, Elsivier etc. In addition to that, she has more than thirty research publications in different conference proceedings. Till the date, she has guided seven M.Tech. and twenty-five B.Tech. research scholars. Now, four Ph.D. scholars, two M.Tech. scholars and seven B.Tech. scholars are working under her guidance. Her research interests include control, renewable energy and microgrid stability and industrial Electronics.